Technique for Fast, Accurate Measurement of Complex Permittivity of EM Materials with Samples of Arbitrary Shape

Isabella Langdon, Martin P. Robinson

School of Physics, Engineering and Technology, University of York, UK
issy.langdon@york.ac.uk, martin.robinson@york.ac.uk

Abstract

This paper presents a novel technique for the measurement of complex permittivity of dielectric materials using samples of arbitrary shape and size. Traditional methods for the use of measuring dielectrics have historically required either large, flat samples of a material, or the material to be in powder form. This is limiting when it comes to modern applications, or in the study of archeological objects. Our approach, based on Resonant Cavity Perturbation theory (RCP), allows for the measurement of small, irregularly shaped samples by combining perturbations from three orthogonal modes in a cuboid cavity. We validate this technique by measuring various materials such as polymers and woods, the results of which demonstrate the effectiveness of the technique in providing reliable dielectric readings at microwave frequencies. This method may be particularly useful in the non-destructive characterization of archeological objects, or in the characterization of new materials.

***Keywords* — complex permittivity, microwave frequencies, non-destructive testing, cavity perturbation, EMC**

I. INTRODUCTION

Dielectric materials are important in electromagnetic compatibility (EMC) because they can affect power losses when used as components or supports for antennas. The permittivity and conductivity of non-metals will alter the resonant frequencies and Q-factors of enclosures, and reliable values of these properties at an appropriate frequency are needed to ensure accurate outputs from computational electromagnetic (CEM) models.

Unfortunately, data on such materials in the literature is often scarce or is presented at, say, 1 MHz or even lower, rather than at the microwave bands that are more relevant to radiated EMC. Novel polymers are constantly being introduced, and the rise of additive manufacturing (3D printing) has led to whole new classes of materials, which will need to be characterized so that they are useful to designers.

Several techniques are available for dielectric measurements [1] including on gases [2], liquids [3], solids [4], biological samples [5] and ceramics [6]. However, they have some drawbacks. Cavity based methods have traditionally required a sample to be formed into a specific geometry, typically a pill-shaped cylinder. Broadband and free-space techniques need large samples, often, for instance when using an open-ended coaxial probe, with a flat surface to make contact with the sensor. It would be very useful to measure the properties of small samples of arbitrary shape.

In this paper we describe a novel technique for measuring the complex permittivity $\varepsilon^* = \varepsilon' - j\varepsilon''$ at a microwave frequency *f,* first proposed by Robinson et al. [11]. The RF conductivity can then be obtained from ε'', while $\varepsilon''/\varepsilon'$ gives the loss tangent. After describing the instrumentation and outlining the RCP theory, we present measurements on a number of useful EM materials.

II. METHOD

The technique is a version of the resonant cavity perturbation (RCP) method [7-10]. Three independent perturbations are measured, each for a mode in which the E-field is strong at the center of the cavity, where the sample sits. However, the directions of the E-fields of the three modes are all mutually orthogonal; combining their perturbations reduces the shape-dependency seen in traditional RCP.

By employing a cuboidal cavity where the dimensions are close in size, but not exactly equal (Table 1, where the frequency for **X** depends on dimensions **Y** and **Z**, and so on), we can arrange for three resonant frequencies also to be close, while being sufficient separated to avoid cross-coupling.

Table 1. Parameters of resonant cavity 4M 2.0

Chamber Dimensions				
	Dimensions (m)	**Freq. ideal (MHz)**	**Freq. actual (MHz)**	**Percent Difference**
X	0.1370	1343.5	1325.98	1.3%
Y	0.1496	1414.2	1367.77	3.3%
Z	0.1677	1484.9	1451.5	2.3%

The remaining uncertainties are reduced still further, by comparing the sample perturbation against that of a replica of the same shape, size, and known ε*.

A. Instrumentation

The previous version of our instrument [11] was used to investigate the possibility of using RCP as a non-destructive method of analyzing archeological objects. We have also reported its use in measuring components of antennas [12].

Several improvements have been implemented in the new instrument. The frequency has been changed from 434 MHz to 1400 MHz. As resonant frequency is inversely proportional to wavelength, this means the cavity is about one third the size, making it lighter and more portable. Furthermore, because the perturbation depends on the ratio of sample volume v_s to cavity

volume v_c, the effect of thermal expansion of the cavity on the measurements should now be less important.

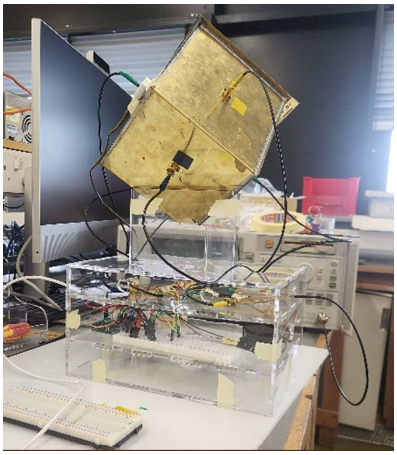

Fig. 1. Resonant cavity 4M 2.0 with VNA and RF switches

As seen in Fig. 1, the cavity is mounted on one corner. A small hole in this corner allows a vertical shaft to pass through to the center of the cavity, where a round table is attached for the sample to be placed on. Both shaft and table are made from low-loss dielectric materials which are accounted for during calibration.

The shaft can be rotated with a motor, allowing the sample support to act as a turntable. This, combined with the rather unusual orientation of the cavity, enables the dipole moment of the sample to rotate with respect to each of the E-field vectors of the three modes. Additional measurements at different turntable angles are intended to reduce the shape dependence even further, although this feature was not implemented in the measurements presented here.

The RF source and detector are an HP8753D vector network analyzer, which automatically calculates resonant frequency and Q-factor from a 1601-point sweep of S21 with an RF power of 5 dBm.

Three pairs of monopole antennas of 18.5mm are attached directly to SMA connectors at the center of each side of the cavity. These SMA connectors attach to a pair of 3-way 600-03-C RF switches via six SMA cables. An Arduino microcontroller, laptop computer and thermal sensor set the VNA sweep range for each mode, upload the resonant frequencies and Q-factors, and record the temperature.

B. Measurement procedure

One side of the cavity is hinged at one edge and connected by an overlapping flange of 16mm at the other three edges, to act as a lid.

To perform a measurement, we open the lid, place the sample or replica centrally on the table, close the lid, and seal it with a single spring clip on each edge except the one with the hinge. The hinged side was designed to lay flush with the box, for good conductivity. Tests were carried out to determine the variation in results when more or less clips are added to the chamber door.

Measurements need to be referenced to the empty cavity (as the resonant frequencies might drift), so each sample is done in the order empty-sample-empty-replica-empty. The values of 'empty' resonant frequency f_0 and Q-factor Q_0 are taken as the mean values of those either side of the sample or replica.

C. Calculation of permittivity

For accurate determination of ε^* a replica is fabricated, e.g. by optical scan followed by 3D printing. Flat replicas can be laser cut if a sheet material of the same thickness is available. We also need the replica permittivity, either from literature value or by measuring it against a known material.

Small differences in volume are corrected for. It is often possible to obtain volume from the scanner's output file, or for simple shapes such as spheres and cylinders, one can calculate from the relevant geometric formula.

The method, including full derivation, has been given in [11] and just a summary of the key steps follows.

To obtain the sample permittivity ε_s^* from that of the replica, we combine measured value resonant frequency, and its corresponding Q-factor, into a single quantity, the complex frequency shift:

$$\Delta\Omega = \frac{\Delta f}{f_0} + \frac{1}{2} j\Delta\left(\frac{1}{Q}\right) \tag{1}$$

where Δf and $\Delta(1/Q)$ are relative to the empty cavity. This quantity depends on ε^*, but also on sample shape, due to the depolarization factor A, as well as sample and cavity volumes. To remove most of the effect of A, we combine the complex frequency shifts for the three measured perturbations:

$$\sum \Delta\Omega^{-1} = \left(\frac{1}{\Delta\Omega_x} + \frac{1}{\Delta\Omega_y} + \frac{1}{\Delta\Omega_z}\right)^{-1} \tag{2}$$

We also use a complex quantity α, the Clausius-Mossotti factor (CMF), which is related to complex permittivity by

$$\alpha = \frac{\varepsilon^* - 1}{\varepsilon^* + 2} \tag{3}$$

To obtain the CMF of the sample α_s from the measured perturbations and the CMF of the replica α_r, while also compensating for non-linear effects, we apply the following:

$$\alpha_s = \alpha_r \frac{p_0 + p_1 \frac{v_c}{v_s \sum \Delta\Omega_s^{-1}} + p_2 \left(\frac{v_c}{v_s \sum \Delta\Omega_s^{-1}}\right)^2}{p_0 + p_1 \frac{v_c}{v_r \sum \Delta\Omega_r^{-1}} + p_2 \left(\frac{v_c}{v_r \sum \Delta\Omega_r^{-1}}\right)^2} \tag{4}$$

where p_0 is zero (to make the permittivity of air exactly 1), and p_1 and p_2 are determined experimentally for a particular cavity as explained in section II.D.

Finally, the sample permittivity ε_s^* is obtained from the sample CMF:

$$\varepsilon_s^* = \frac{1 + 2\alpha_s}{1 - \alpha_s} \tag{5}$$

D. Calibration

The new cavity was calibrated to set the values of p_1 and p_2 as in [11]. Two known materials plus air were sufficient to

define the non-linear curve for the range of permittivities in this study. If in future measurements are to be made of much higher values, the instrument should be checked with additional calibration standards.

Here the standards were air (ε'=1.00) and several spheres of PTFE (ε'=2.10) and quartz (ε'=3.90). Volumes were 8.6 cm^3 and 9.3-10.2 cm^3 respectively. Perturbations were measured 9 times for the PTFE and 14 times for the quartz, and a second-order polynomial fitted by means of the 'polyfit' function in Matlab. The new p_1 was found to be -0.1192 + 0.0014j and the new p_2 was -0.5693 + 0.0023j. As a check, ε' values of the PTFE standards were then calculated to be in the range 2.095-2.102, while the quartz standards were 3.874-3.960. This demonstrates that the calibration was successful and the measurements of the standards are repeatable.

III. Measurements

A. Factors affecting measurement

There are several factors that may affect the measurement results when operating 4M 2.0. Namely, the position and orientation of the objects within the chamber, and the seal of the chamber door. To test how seal integrity affects the results, a study was conducted, in which the number of clips holding each edge of the door was varied. To investigate how much variation in sample position is acceptable, a further study was done in which the sample was placed in offset positions as well as the centre.

B. Verowhite and PTFE

To test 4M 2.0, we retested a series of previously examined objects, the permittivities of which are known. This is a set of five objects of various geometrical shapes, made in both Verowhite, a 3D-printed polymer, and in PTFE (Teflon).

C. Acrylic versus PTFE

We then used the new cavity to obtain the permittivity of acrylic (polymethyl methacrylate, PMMA) by comparing acrylic and PTFE spheres, diameter approximately 25mm. Samples were labeled Acrylic 1 and Acrylic 2, PTFE 1 and PTFE 2. Samples were then compared and cross compared with each other, to ensure that the results were reliable (Table 5).

D. Polymers and woods versus acrylic

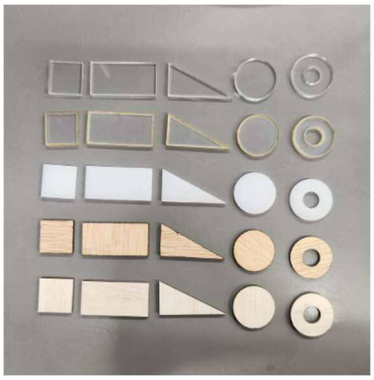

Fig. 2. Samples, top to bottom, Acrylic, Polycarbonate, Acetal, Plywood, Balsawood. Shapes are left to right, Square, Rectangle, Triangle, Disc, Tube

To further test the method, we measured samples made from five different shapes of 3mm thickness, including one with a sharp point and another with a hole. These can be seen in Figure 3; the left hand objects are 20mm squares. The materials tested were three types of plastic: acetal, polycarbonate and acrylic, and two types of wood: plywood, balsawood.

As we had already found the dielectric properties of acrylic, we used that as our reference for each of the others. Each of the tests were only conducted once, apart from the square samples which were tested 3 times and an average taken.

IV. Results

A. Factors affecting measurement

The results of the seal test can be seen in Table 2.

Table 2. PTFE medium tube (Replica) vs Verowhite Medium Tube (sample) with varying numbers of clips on the door

Seal Testing				
Number of Clips	**ε'**	**ε''**	**Standard Deviation ε'**	**Standard Deviation ε''**
0	1.9973	0.0239	0.0362	0.0158
3	2.0053	0.0197	0.0028	0.0017
9	1.9505	0.0185	0.0065	0.0005

Table 2 shows a minor variation of 2.5% in ε', but a 25% difference between 0 and 3 clips, showing there is a lack of electrical conductivity without sealing the door. However, there is only a 6.2% difference in ε'' between 3 and 9 clips. As a standard, 3 clips were used when conducting measurements due to the time-consuming nature of removing and adding 9 clips for every measurement.

Objects placed offset from the centre of the chamber give the results shown in Table 3. This shows that although the procedure was to place the sample at the centre where the E-field is strongest, small misplacements do not adversely affect the measurements.

Table 3. PTFE medium tube vs Verowhite medium tube placement variation tests. Variation was calculated from the centre.

Off-centre Testing				
Placement on turntable	**ε'**	**ε''**	**Standard Deviation ε'**	**Standard Deviation ε''**
Centre	2.005	0.0197	0.0028	0.0017
Left	1.994	0.015	0.2599	0.0008
Right	1.981	0.0167	0.0467	0.0017
Back	1.927	0.0133	0.0094	0.0014
Front	2.001	0.017	0.0068	0.0008

B. Verowhite versus PTFE

Table 4 shows comparative results between samples measured using 4M [11] and then 4M 2.0. We see good agreement in results, with low standard deviation in both ε' and ε'', though slightly higher for ε''

Table 4. PTFE vs Verowhite shape results compared to results using previous cavity, 4M

Verowhite vs PTFE Testing							
		4M 2.0		4M		Standard Deviation 4M 2.0	
Sample	**Replica**	**ε'**	**ε''**	**ε'**	**ε''**	**ε'**	**ε''**
Verowhite cone	PTFE Cone	2.799	0.064	2.818	0.051	0.0098	0.0064
Verowhite Hollow tube	PTFE Hollow Tube	3.052	0.085	3.137	0.058	0.0427	0.0134
Verowhite small tube	PTFE Small Tube	2.954	0.068	3.034	0.042	0.0397	0.0129
Verowhite medium tube	PTFE medium tube	3.016	0.073	3.106	0.052	0.0451	0.0105
PTFE Cone	Verowhite cone	2.106	-0.003	2.201	0.005	0.0476	0.0009
PTFE Hollow Tube	Verowhite Hollow tube	2.015	-0.006	2.050	0.002	0.0175	0.0027
PTFE Small Tube	Verowhite small tube	2.031	-0.016	2.093	-0.003	0.0309	0.0095
PTFE medium tube	Verowhite medium tube	2.005	0.0197	2.063	0.0002	0.0288	0.0099

Figure 3 shows the comparative results given in Table 4. We see a good correlation on ε', but less so in ε". This may be related to the different operating frequencies of the cavities.

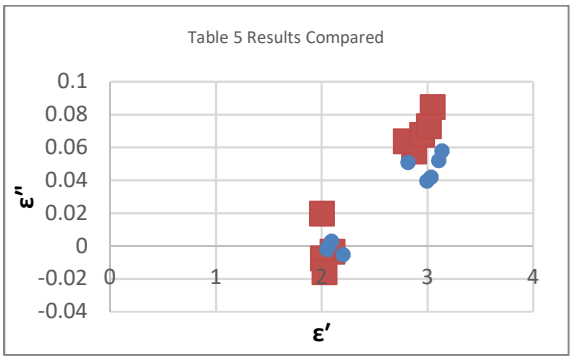

Fig. 3. 4M results (blue circles) vs 4M 2.0 results (red squares) for PTFE and Verowhite

C. *Acrylic versus PTFE*

Table 5. Comparing two PTFE spheres and two Acrylic spheres

Acrylic versus PTFE			
Sample	**Replica**	**ε'**	**ε''**
Acrylic 1	PTFE 1	2.639	0.018
Acrylic 2	PTFE 2	2.675	0.017
Acrylic 1	PTFE 2	2.643	0.016
Acrylic 2	PTFE 1	2.651	0.014
Average		2.652	0.016
Standard Deviation		0.0445	0.006

The comparison of acrylic and PTFE sphere is shown in Table 5. The results presented show very minor variation in ε', and a relatively small variation in ε". Again, when considering the standard deviation, we see repeatable results. This shows stability in the measurements being taken.

D. Polymers and woods versus acrylic

The results on the plastic and wood shapes can be found in Table 7 and are plotted in Figure 4, showing that the real part of the permittivity (ε') was consistent across different shapes, with a variation of less than 3.5%. However, we see the imaginary part (ε") exhibited larger variations in percentage terms, particularly for the higher loss materials such as plywood and acetal. We attribute these variations to the small magnitude of the ε" values, i.e. the materials are all low-loss dielectrics, so a small absolute change in ε" corresponds to a large percentage difference. Nevertheless, the method proves to be useful in distinguishing materials and evaluating their behaviour in the presence of EM fields at microwave frequencies.

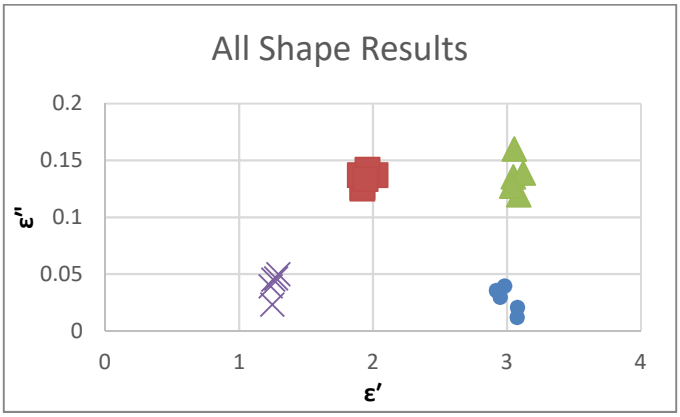

Fig. 4. Measured permittivity of Polycarbonate (blue circles), Balsawood (purple crosses), Plywood (red squares) and Acetal (green triangles) for all five shapes

Table 7. Variation of dielectric properties with shape

Shape and Material Testing								
Sample	**Plywood**		**Acetal**		**Polycarbonate**		**Balsawood**	
	ε'	**ε''**	**ε'**	**ε''**	**ε'**	**ε''**	**ε'**	**ε''**
Square	1.92	0.13	3.01	0.14	2.92	0.04	1.28	0.05
Triangle	1.92	0.13	3.05	0.16	3.08	0.01	1.26	0.05
Tube	1.91	0.14	3.09	0.12	2.98	0.04	1.25	0.02
Rectangle	2.02	0.14	3.12	0.14	3.08	0.02	1.29	0.05
Disc	1.96	0.14	3.04	0.13	2.95	0.03	1.24	0.04
Average	1.95	0.13	3.05	0.14	3.00	0.03	1.26	0.04
Standard Deviation	0.041	0.015	0.032	0.014	0.065	0.010	0.021	0.009

V. Discussion

A. RCP Technique

Once the replicas have been made, RCP is a rapid, accurate measurement. It is non-invasive, using low power RF, which will not heat up or damage the sample.

It is surprising that the hinged lid works so well and does not require a gasket – this makes the measurement faster than before. In our previous cavity the sample was introduced through a hole in the top lid, which was awkward and restricted the sample size.

The offset error is small, so the operator can position sample and replica by eye. This is because the E-field has cosine dependency, so will not change rapidly until close to the side. For more complicated shapes, taking a photograph of the sample on the turntable assists with putting the replica in the same position.

The technique is narrowband, however, the dielectric properties of many EM materials vary quite slowly with frequency. To make measurements in other bands of the spectrum, larger or smaller cavities could be constructed.

B. Properties of EM materials

Table 9. Summary of dielectric properties for all measured materials

Complex permittivity of all materials					
Material	**Mean ε'**	**STD ε'**	**Mean ε''**	**STD ε''**	**Notes**
Verowhite	2.96	0.014	0.072	0.0028	Compared against PTFE replicas
PTFE	2.04	0.012	0.001	0.003	Compared against Verowhite Replicas
Acrylic	2.65	0.045	0.016	0.006	Replica for next 4 materials
Plywood	1.95	0.485	0.13	0.015	High loss
Acetal	3.05	0.032	0.14	0.014	High loss
Polycarb.	3.00	0.065	0.030	0.010	Low loss tangent
Balsawood	1.26	0.021	0.040	0.009	Low density, low dielectric constant

The results of all the materials studies are summarised in Table 9. The measured values of Verowhite (ε' = 2.96, ε'' = 0.072) at 1400MHz compare well with previously reported values at 430 MHz of ε' = 2.94, ε'' = 0.0772 [11] and at mm-wave frequencies (85-105 GHz) of ε' = 2.81, ε'' = 0.0555 [13]. This consistency across a wide frequency range validates the accuracy of the measurement technique and confirms that this particular 3D-printed material has a relatively high loss tangent compared to traditional materials used in antenna design. The values for the other polymers tested are also consistent with literature values [14].

Of the materials listed in Table 7, plywood and acetal have higher loss, so will also be worse when positioned near antennas, but are potentially better for use inside enclosures, as they will damp the internal resonances and improve shielding effectiveness.

Balsa has the lowest dielectric constant, as expected from its low density. Polycarbonate has the lowest loss tangent tanδ. Both would be good for antennas components and supports.

These measurements show that types of wood or plastic that look similar can have very different dielectric properties, so it is important to be able to measure them.

C. Further work

In the work presented here, the sample (and replica) remained static while the perturbations were measured. By rotating the sample to different positions, using the turntable, further independent measurements can be done, which we believe should reduce the uncertainties. We would need to investigate the tradeoff between this improvement and the longer measurement time.

To make the method more convenient, we will investigate replacing the physical replica with a simulation implemented in a CEM model. Our most recent results show that the required degree of similarity between replica and sample is less stringent than we initially expected, which makes the technique practically more attractive.

We plan to replace the current analyzer with a smaller, more portable VNA, which will also reduce the cost. RCP does not rely on phase measurements, so one could instead use a simpler and cheaper combination of swept frequency source and separate detector.

It would be interesting to test EMC materials that are intended to have high loss, such as radio absorbing material (RAM), carbon-loaded polymers etc. Our previous experience with other types of RCP sensor shows that they can measure lossy liquids such as saline solutions [8]. The loaded Q of the cavity could go much lower without the system losing track of

the resonances, so should be capable of measuring much higher loss tangents than those presented here.

Wider applications in the heritage sector include distinguishing genuine items from fakes, controlling banned materials such as ivory (which could be passed off as bone or teeth from other animals) as well as identifying artefacts from digs or in museum collections.

D. Limitations of Method

The size of the chamber is relatively small, with larger archaeological samples unable to be tested in the chamber. Similarly, very small samples do not measure well due to the high uncertainties. To address this, two more chambers, one half the size and the other double the size, are in production, to allow a greater range of measurements to be taken. We have not yet systematically explored the upper limitations of the real and imaginary parts of the permittivity (dielectric constant and loss factor). However, initial tests on high-loss materials found consistent results across different sample volumes.

VI. Conclusion

The technique described here is an improvement on traditional RCP that eliminates the need for a sample of a specified geometry. It provides fast, accurate measurement of both dielectric constant and loss factor at microwave frequencies appropriate to EMC testing and will give better input data for CEM models.

Our method has been shown to work on a number of different shapes and materials, showing good repeatability and low uncertainties. Furthermore, the permittivity values of those materials add to our knowledge base. This will help designers reduce antenna losses and understand the effect of dielectric materials on enclosure resonances. It will be useful for rapid characterization of new materials produced by modern processes such as additive manufacturing.

The novel method described here will have wider applications including in environment, heritage and archaeology, as well as being helpful in the field of EMC design and testing.

Acknowledgments

The authors thank Mr Christopher Gordon, formerly of the University of York for updating the Python code and making it suitable for the new cavity. They also thank the Technical Support Staff of the School of PET, University of York for assistance making the samples and fabricating the cavity.

References

[1] Kaatze, U, 2012. Measuring the dielectric properties of materials. Ninety-year development from low-frequency techniques to broadband spectroscopy and high-frequency imaging. Measurement Science and Technology, 24(1), p.012005.

[2] J. F. Rouleau, J. Goyette, T. K. Bose, and M. F. Frechette. Investigation of a microwave differential cavity resonator device for the measurement of humidity in gases. Review of Scientific Instruments, 70:3590–3594, 1999.

[3] A. P. Gregory and R. N. Clarke. A review of RF and microwave techniques for dielectric measurements on polar liquids. IEEE Transactions on Dielectrics and Electrical Insulation, 13(4):727–743, 2006

[4] C. N. Works, T. W. Dakin, and F. W. Boggs. A resonant-cavity method for measuring dielectric properties at ultrahigh frequencies. Electrical Engineering, 63(12), 1944

[5] M P Robinson, I D Flintoft, L Dawson, J Clegg, J G Truscott and X Zhu 2010, 'Application of Resonant Cavity Perturbation to in-vivo Segmental Hydration Analysis' Meas. Sci. Technol. 21 pp 015804.1-015804.10

[6] Trans-Tech Inc. Dielectric Resonators—A Designer Guide to Microwave Dielectric Ceramics, rev. 2 edition, 1990. Publication No. 50080040.

[7] Horner F, Taylor T A, Dunsmuir R, Lamb J and Jackson W 1946. 'Resonance methods of dielectric measurement at centimetre wavelengths.' J. IEE 93 III pp53-68

[8] Kraszewski, A. W., Nelson, S. O. and You, T. S., 1990. Use of a microwave cavity for sensing dielectric properties of arbitrarily shaped biological objects. IEEE Transactions on Microwave Theory and Techniques, 38(7), pp.858-863.

[9] Harrington R F 1961, Time Harmonic Electromagnetic Fields, Wiley, New York, Ch. 7.

[10] Kraszewski A W and Nelson S O 1996. 'Resonant cavity perturbation: some new applications of an old measuring technique' J. Microwave Power vol. 31, pp 178-187.

[11] M P Robinson, L C Fitton, A Little, S N Cobb and S P Ashby 2019, 'Dielectric replica measurement: a new technique for obtaining the complex permittivity of irregularly shaped objects' Meas. Sci. Technol. 30 045902 (12pp)

[12] J. F. Dawson, S. J. Bale, M. P. Robinson, T. Rees, B. J. Petit, R. Hoad and M. Hough 2024 'A Pulse Antenna Suite for IEMI Testing' IEEE Electromagnetic Compatibility Magazine – Volume 13 – Quarter 3, 40-53

[13] Bur, A. J., 1985. Dielectric properties of polymers at microwave frequencies: a review. Polymer, 26(7), pp.963-977

[14] Choi, H. E. and Choi, E., 2024. High-Precision complex permittivity measurement of high loss dielectric materials using a geometrical gap in millimeter wave frequency. Journal of Infrared, Millimeter, and Terahertz Waves, 45(1), pp.97-115.